

## Sumanenylferrocenes and their solid state self-assembly

*Berit Topolinski, Bernd M. Schmidt, Shuhei Higashibayashi, Hidehiro Sakurai  
and Dieter Lentz*

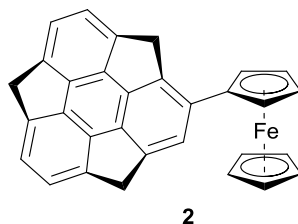
Supporting Information

### Chemical Syntheses and Compound Characterization

#### General

All experiments were carried out under standard Schlenk conditions and argon atmosphere, 1,2-dichloroethane (DCE) was distilled from phosphorus pentoxide, THF was distilled from potassium, both were stored over molecular sieve (3 Å). Melting points were determined on a Stanford Research Systems MPA100 (**2**) or on a Gallenkamp Melting Point Apparatus (**3**) and are uncorrected. IR spectra were recorded on a Nicolet iS10 MFR FT-IR Sp spectrometer (signals are denoted as following, s (strong), m (middle) and w (weak)). <sup>1</sup>H, <sup>19</sup>F and <sup>13</sup>C NMR spectra were measured on JEOL ECS 400/500 spectrometer or on a Bruker Instruments AVIII 700 at 23 °C. CDCl<sub>3</sub> and CD<sub>2</sub>Cl<sub>2</sub> were used as solvents and the residual solvent peak was taken as an internal standard (<sup>1</sup>H NMR: CDCl<sub>3</sub> 7.26; <sup>13</sup>C NMR: CDCl<sub>3</sub> 77.0; CD<sub>2</sub>Cl<sub>2</sub> 54.00 ppm always proton-decoupled). High resolution mass spectra (HRMS) were measured on a JEOL JMS-777V or on a MAT CH7A spectrometer using electron impact ionization method (EI). TLC analysis was performed using Merck Silica gel 60 F254 and PTLC was conducted using Wako Wakogel B-5F. All reagents and solvents were commercially purchased and used as received. 1,1'-Dibromoferrocene was synthesized according to literature procedure.<sup>[S1]</sup>

## Sumanenylferrocene (2)

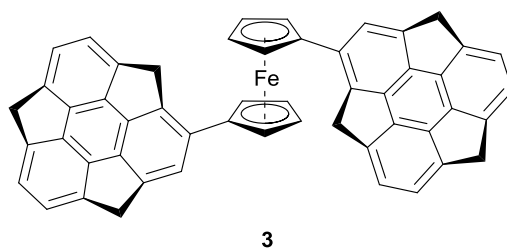


In a 20 mL Schlenk tube ferrocene (43 mg, 0.23 mmol, 4.0 eq) and potassium *tert*-butoxide (3 mg, 0.02 mmol, 0.4 eq) were dissolved in 2 mL anhydrous THF. After cooling to -40 °C *tert*-butyllithium (0.2 mL, 1.3 M in hexane, 5.0 eq) was added dropwise and formation of a red precipitate was observed. After one hour at the same temperature anhydrous zinc chloride (52 mg, 0.38 mmol, 7.0 eq) dissolved in 2 mL dry THF was added drop-wise. The orange solution was stirred for another 30 minutes at -40 °C and then for 30 minutes at room temperature. This solution was transferred to a 20 mL chemstation tube containing monoiodosumanene (22 mg, 0.06 mmol, 1.0 eq), palladium(II) acetate (0.3 mg, 3 mol%) and triphenylphosphine (0.8 mg, 6 mol%) under argon. The reddish solution was heated at 70 °C for three days in a chemstation. Afterwards the red-brown solution was transferred to a flask and the solvent was removed. PTLC on silica gel with hexane/dichloromethane (1:1) yielded 11 mg of an orange solid (third fraction). Final purification using a recycling GPC (chloroform as eluting solvent) yielding 10 mg (38%) as an orange powder. Crystals suitable for X-ray analysis were grown by slow evaporation of a dichloromethane solution.

**<sup>1</sup>H-NMR (500 MHz, CDCl<sub>3</sub>):**  $\delta$  = 7.33 (s, 1H), 7.10-7.06 (m, 4H), 4.79 - 4.73 (m, 4H), 4.58 (s, 1H), 4.35 (s, 1H), 4.30 (s, 1H), 4.13 (s, 5H), 3.53 - 3.38 ppm (m, 3H). **<sup>13</sup>C-NMR (125 MHz, CDCl<sub>3</sub>):**  $\delta$  = 135.86 (s, C<sub>ipso(sum)</sub>), 123.44 (s, CH<sub>arom</sub>), 123.28 (s, CH<sub>arom</sub>), 123.09 (s, CH<sub>arom</sub>), 122.94 (s, CH<sub>arom</sub>), 121.71 (s, CH<sub>arom</sub>), 149.53 (s, C<sub>flank</sub>), 149.15 (s, C<sub>flank</sub>), 149.10 (s, C<sub>hub</sub>), 149.00 (s, C<sub>flank</sub>), 148.71 (s, C<sub>hub</sub>), 148.67 (s, C<sub>hub</sub>), 148.60 (s, C<sub>flank</sub>), 168.57 (s, C<sub>hub</sub>), 148.49 (s, C<sub>flank</sub>), 148.37 (s, C<sub>hub</sub>), 146.76 (s, C<sub>hub</sub>), 144.29 (s, C<sub>flank</sub>), 85.50 (s, C<sub>ipso(Cp)</sub>), 69.64 (s, C<sub>Cp</sub>), 67.82 (s, C<sub>Cp(sub)</sub>), 67.66 (s, C<sub>Cp(sub)</sub>), 42.65 (s, CH<sub>2</sub>), 41.68 (s, CH<sub>2</sub>), 41.52 ppm (s, CH<sub>2</sub>). **EI-MS:**  $m/z$  = 448 (100 %, [M]<sup>+</sup>), 326 (14 %, [Cp-Sum]<sup>+</sup>), 224 (8 %, [M]<sup>2+</sup>). **HR EI-MS:**  $m/z$  = 448.0926 (found), 448.0914 (calc'd). **FT-IR:**  $\nu$  = 3094 (w), 3040 (w), 2897 (w), 2424 (w), 2244 (w), 1720 (w), 1633 (w), 1563 (w), 1489 (w), 1452 (w), 1395 (m), 1377 (w), 1343 (w), 1260 (w), 1260 (w), 1229 (w), 1179 (w), 1149 (w), 1075 (w), 1032 (m), 998 (m),

921 (w), 902 (m), 826 (m), 807 (w), 783 (s), 755 (vw), 730 (m), 682 (w), 664 (w), 644 (w), 609 (m), 590 (vw), 559 (vw), 535  $\text{cm}^{-1}$  (vw). **Mp:** 219 °C (decomposition).

### Disumanenylferrocene (3)



1,1'-Dibromoferrocene (18 mg, 51.3  $\mu\text{mol}$ , 1.0 eq) was dissolved in 0.5 mL dry THF in a 25 mL Schlenk tube. The orange solution was cooled to -30 °C. *n*-Butyllithium (0.1 mL, 2.5 M in hexane, 5.0 eq) was added, orange precipitate appeared and stirring at -30 °C was continued for 30 minutes. After stirring for 15 minutes at room temperature the precipitate dissolved and the red solution was again cooled to -30 °C. Anhydrous zinc chloride (21 mg, 0.15 mmol, 3.0 eq) was added at once. After stirring at -30 °C for 30 minutes and at room temperature for 30 minutes, palladium(II) acetate (0.6 mg, 5 mol%) and triphenylphosphine (1.3 mg, 10 mol%) were added. Monoiodosumanene (44 mg, 0.11 mmol, 2.2 eq) was dissolved in 1 mL dry THF and added *via* syringe. The Schlenk tube was sealed and heated in an oil bath for 24 hours at 70 °C. Afterwards the solvent was removed; column chromatography on silica gel was conducted with pentane/dichloromethane (3:1) as eluting solvents which yielded 4 mg (11%) of the red product as the last (fifth) fraction. Crystals suitable for X-ray analysis were grown from a 1:1 mixture of chloroform and dichloromethane by slow evaporation.

**$^1\text{H-NMR}$  (400 MHz,  $\text{CDCl}_3$ ):**  $\delta$  = 7.07 (d,  $^3J$  = 6.3 Hz, 1H), 7.03 - 6.84 (m, 3H), 6.79 (d,  $^3J$  = 6.6 Hz, 1H), 5.29 - 4.84 (br, 3H), 4.78 - 4.59 (br, 1H), 4.59 (d,  $^2J$  = 19.3 Hz, 1H), 4.51 (d,  $^2J$  = 19.3 Hz, 1H), 4.31 - 4.11 (br, m, 1H), 3.67 - 3.44 (br, 1H), 3.22 (d,  $^2J$  = 19.4 Hz, 1H), 3.10 ppm (d,  $^2J$  = 19.3 Hz, 1H).  **$^{13}\text{C-NMR}$  (175 MHz,  $\text{CD}_2\text{Cl}_2$ ):**  $\delta$  = 149.25 (s,  $\text{C}_{\text{flank}}$ ), 149.07 (s,  $\text{C}_{\text{flank}}$ ), 148.72 (s,  $\text{C}_{\text{hub}}$ ), 148.63 (s,  $\text{C}_{\text{hub}}$ ), 148.58 (s,  $\text{C}_{\text{hub}}$ ), 148.49 (s,  $\text{C}_{\text{hub}}$ ), 148.38 (s,  $\text{C}_{\text{flank}}$ ), 148.29 (s,  $\text{C}_{\text{flank}}$ ), 148.23 (s,  $\text{C}_{\text{flank}}$ ), 148.15 (s,  $\text{C}_{\text{flank}}$ ), 148.05 (s,  $\text{C}_{\text{hub}}$ ), 123.76 (s,  $\text{CH}_{\text{arom}}$ ), 123.62 (s,  $\text{CH}_{\text{arom}}$ ), 123.52 (s,  $\text{CH}_{\text{arom}}$ ), 123.23 (br s,  $\text{CH}_{\text{arom}}$ ), 122.98 (br s,  $\text{CH}_{\text{arom}}$ ),

71.28 (br s, C<sub>Cp(sub)</sub>), 68.30 (br s, C<sub>Cp(sub)</sub>), 42.20 (s, CH<sub>2</sub>), 41.69 (s, CH<sub>2</sub>), 41.66 ppm (s, CH<sub>2</sub>). Due to the very low solubility of **3** the signals for both *ipso*-carbons and one hub carbon could not be assigned. **EI-MS**: m/z = 710 (100 %, [M]<sup>+</sup>), 326 (15 %, [Cp-Sum]<sup>+</sup>). **HR EI-MS**: m/z = 710.1705 (found), 710.1697 (calc'd). **FT-IR**:  $\nu$  = 3098 (w), 3044 (vw), 2921 (m), 2853 (w), 2360 (w), 2246 (vw), 1862 (vw), 1725 (w), 1637 (w), 1572 (w), 1492 (vw), 1455 (w), 1395 (w), 1379 (w), 1346 (vw), 1261 (w), 1232 (vw), 1208 (vw), 1181 (w), 1152 (vw), 1109 (vw), 1080 (w), 1036 (w), 1000 (w), 966 (vw), 922 (w), 904 (w), 828 (vw), 786 (m), 756 (vw), 731 (m), 683 (vw), 665 (vw), 646 (vw), 610 cm<sup>-1</sup> (m). **Mp**: 158 °C (decomposition).

## Cyclic Voltammetry

Cyclic voltammetry was measured on a ALS/CH Instruments Electrochemical Analyzer Model 620c using a Schlenk measuring cell with three platinum wires as electrodes. Measurements were conducted in dry THF with tetra-*n*-butylammonium hexafluorophosphate (0.1 M) as conducting salt, an substance concentration of  $5 \cdot 10^{-4}$  M and a scan rate of 0.1 V/s (if not mentioned otherwise). Decamethylferrocene was used as an internal standard (~of  $5 \cdot 10^{-4}$  M). In our setup decamethylferrocene was found to be -0.48 V against ferrocene.

Compound	$E_0$ ( $E_{\text{red}}$ (*)) vs Decamethylferrocene in V	$E_0$ ( $E_{\text{red}}$ (*)) vs ferrocene in V
2	0.450 -2.539* (irrev) -2.867* (irrev)	-0.030 -3.019* (irrev) -3.347* (irrev)
3	0.430 -2.427* (irrev) -2.906* (irrev)	-0.050 -2.907* (irrev) -3.386* (irrev)

**Table S1:** Redoxpotentials ( $E_0 = (E_{\text{ox}} + E_{\text{red}})/2$ ) and reductionpotentials of **2** and **3**; irrev = irreversibile reduction.

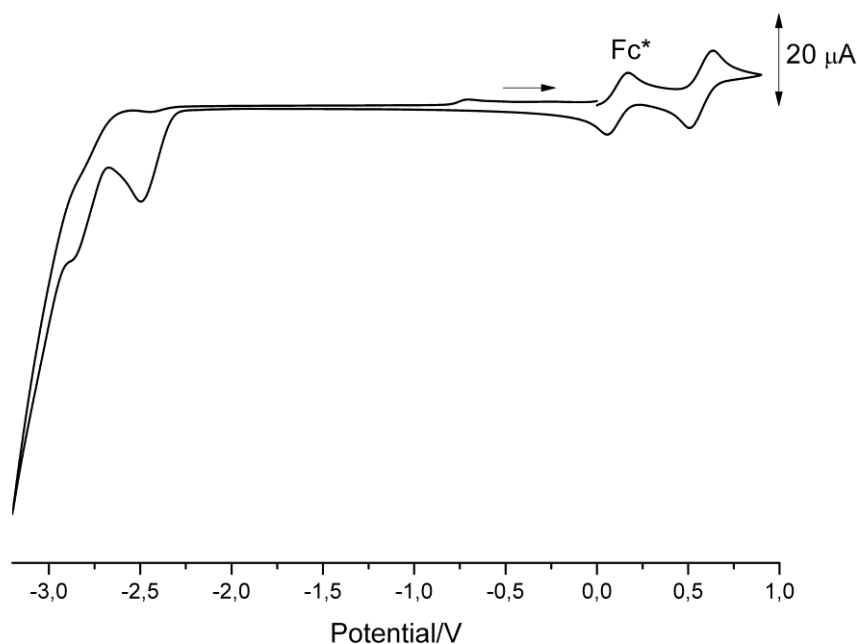


**Figure S1.** Cyclic voltammetry measurement of **2**.

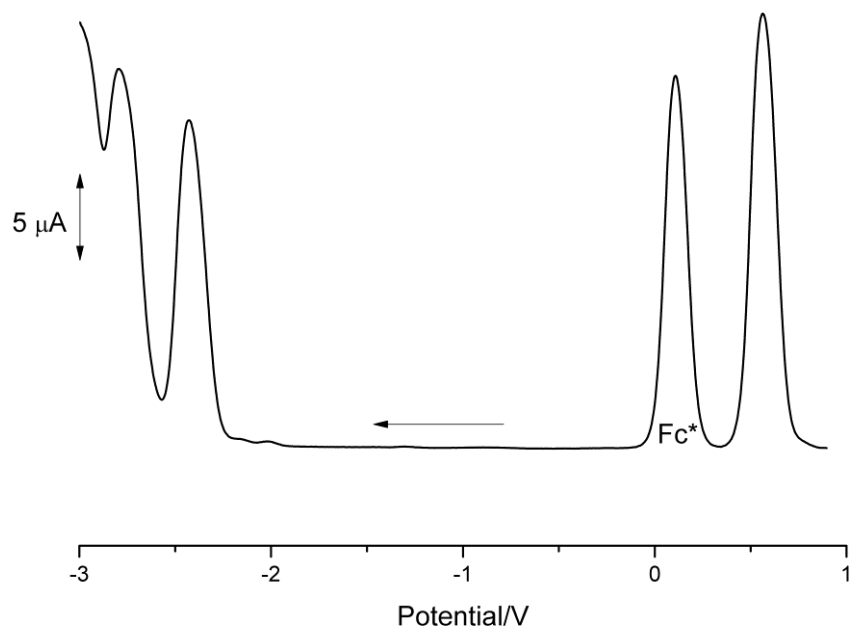


**Figure S2.** Square wave measurement of **2**.

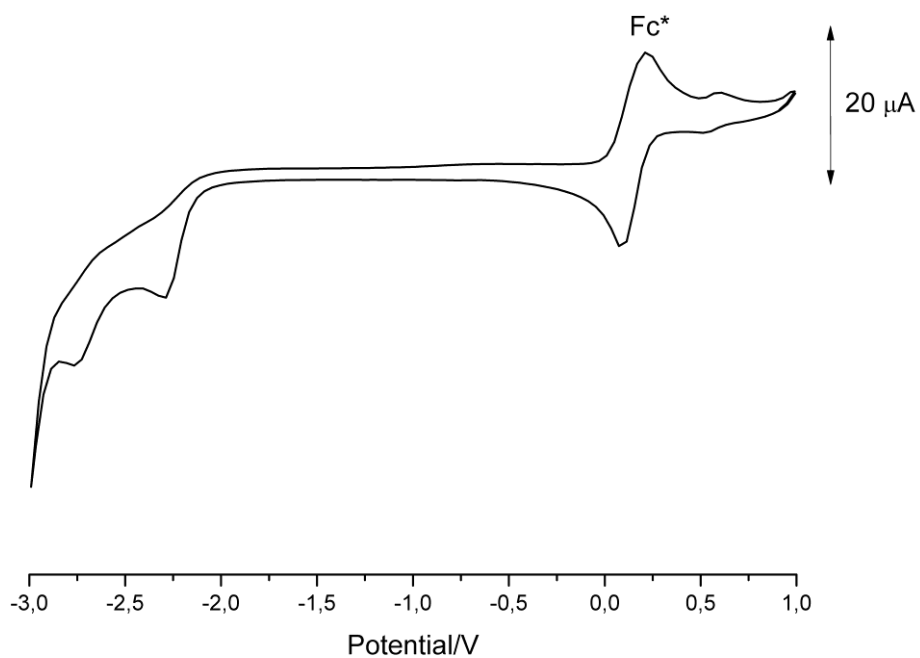


**Figure S3.** Cyclic voltammetry measurement of **3**. Scan rate 0.05 V/s. The intensity of the redox waves is very low due to poor solubility of **3**.

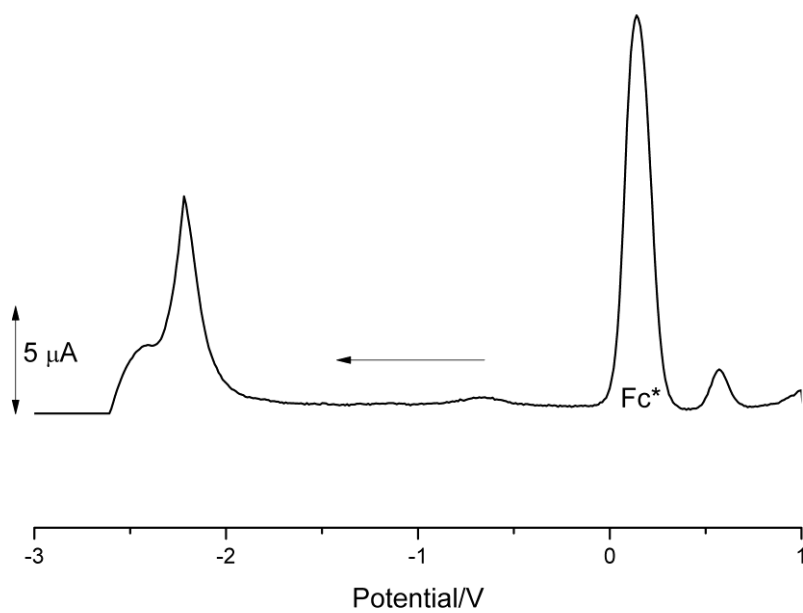


**Figure S4.** Square wave measurement of **3**.

## Crystal Structures

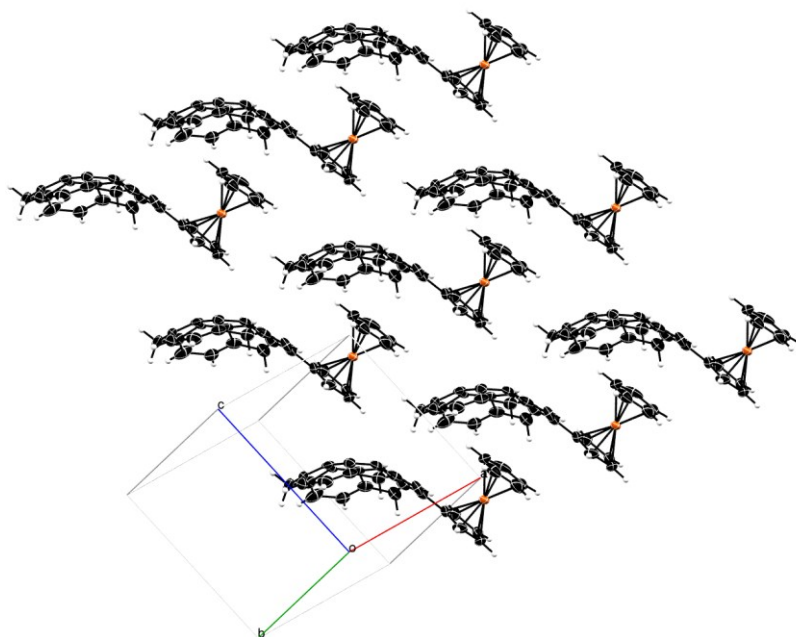


**Figure S5.** Packing of **2** with respect to the cell coordinates (a: red, b:green, c:blue).

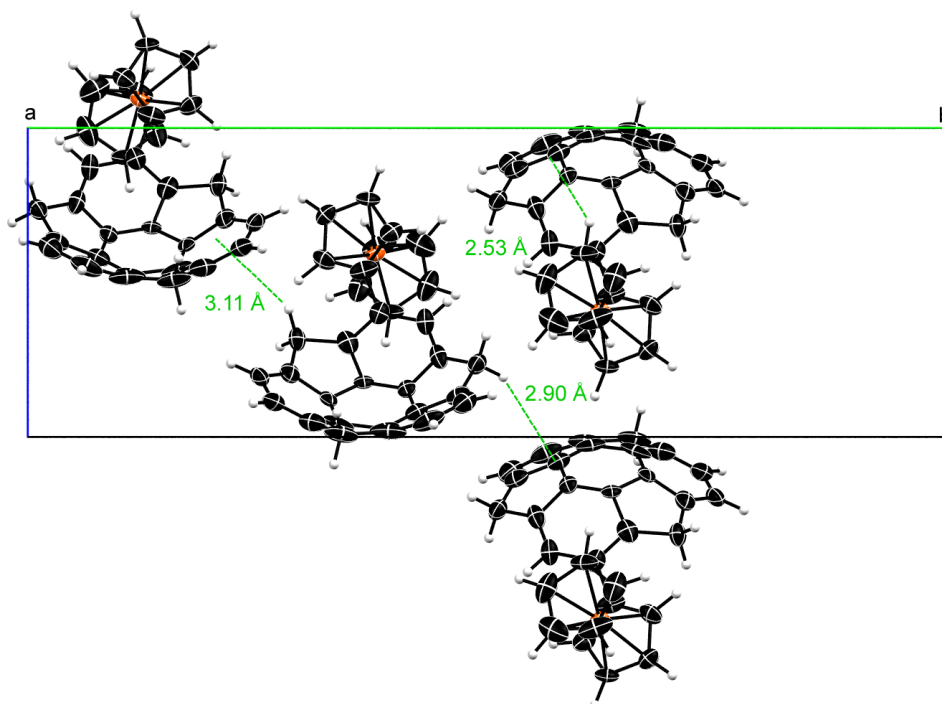


**Figure S6:** View on a part of the unit cell of **2**, showing the interactions described in the main text page 2.

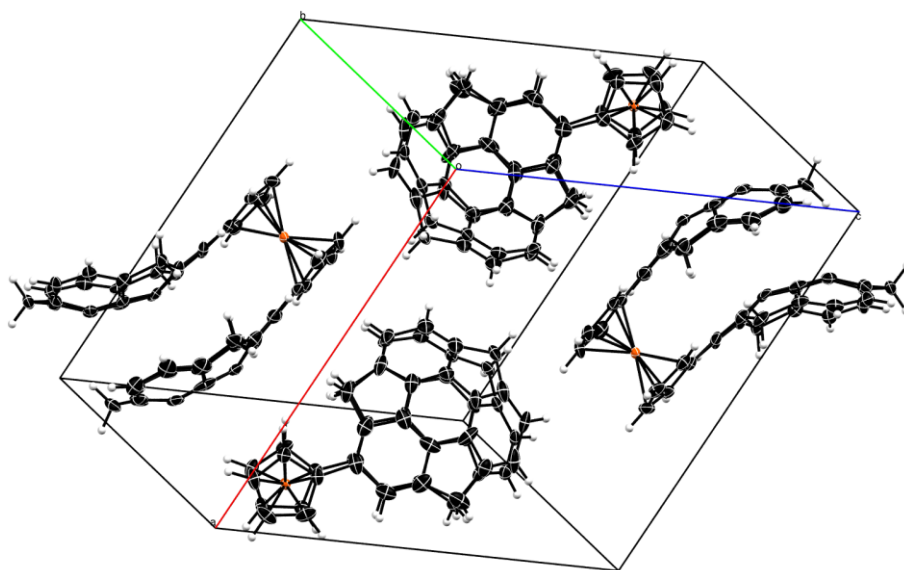


**Figure S7.** Unit cell of compound **3**.

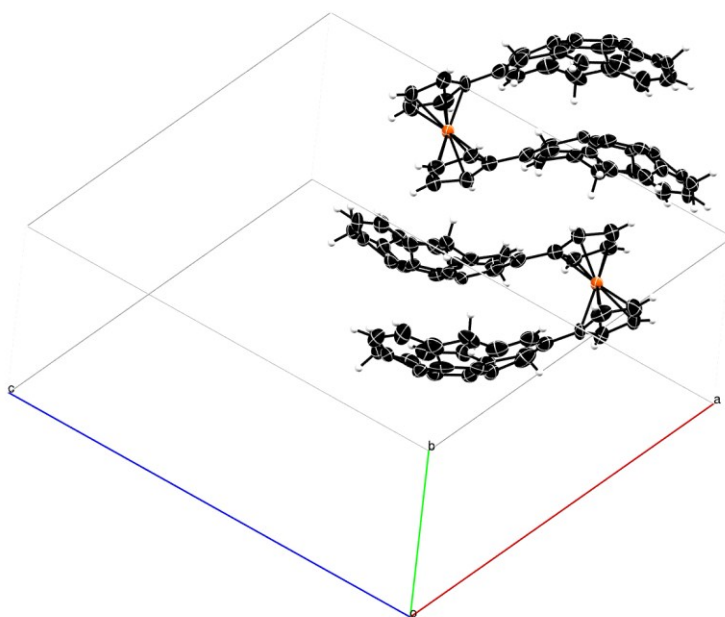


**Figure S8.** 'Dimeric' unit of **3** with respect to the cell coordinates.

## Computational Details

The optimization of the structures of **2** and **3** was carried out using the Gaussian 09 program, using gas-phase density functional theory calculations at wB97XD/6-31G(d,p) level for C, H and lan12dz for Fe, level of theory. Images were generated using GaussView 5.0.9, electrostatic potential maps were generated using an isovalue of 0.0004 in the range from  $-2.500e^{-2}$  to  $2.00e^{-2}$ .

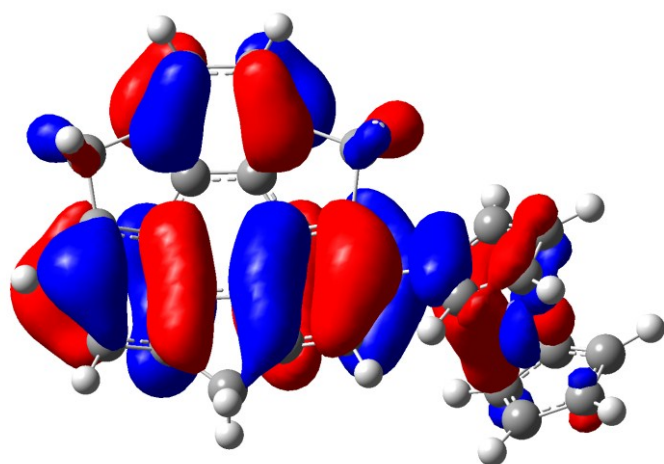


**Figure S9.** Visualization of the HOMO of **2**

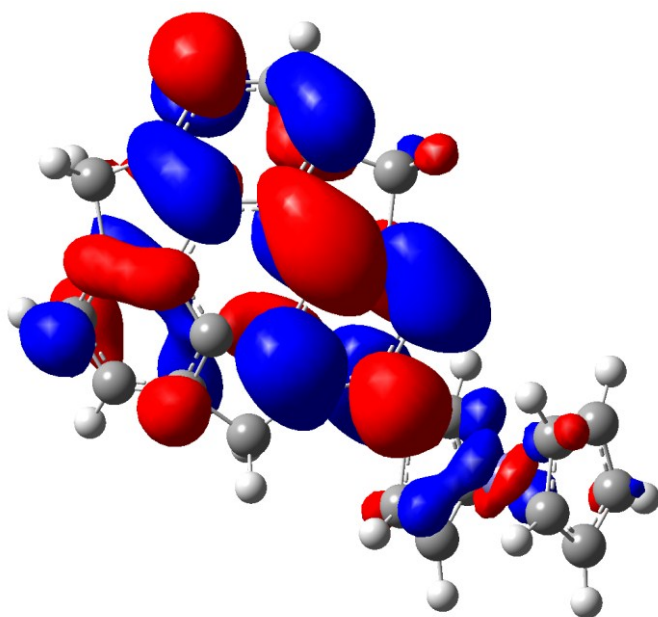


**Figure S10.** Visualization of the LUMO of **2**

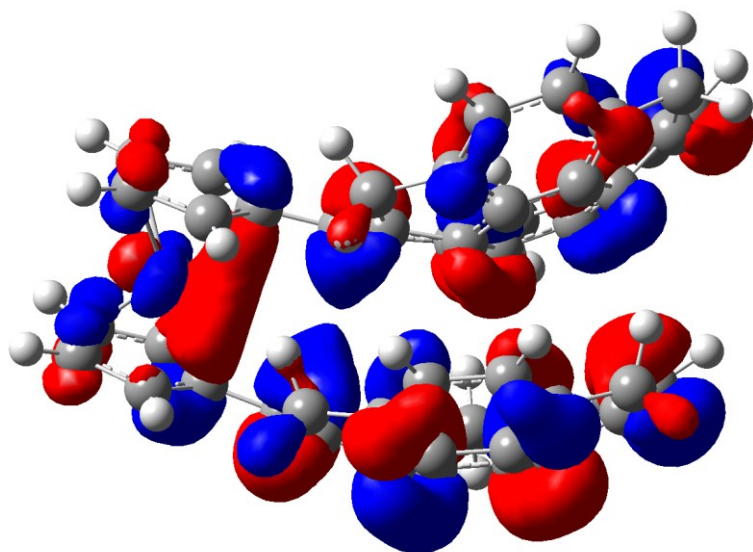


**Figure S11.** Visualization of the HOMO of **3**

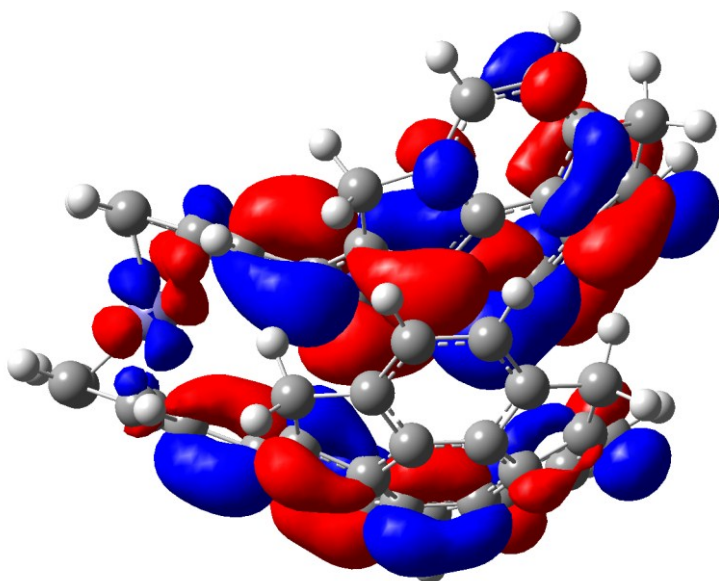


**Figure S12.** Visualization of the LUMO of **3**

negative  positive

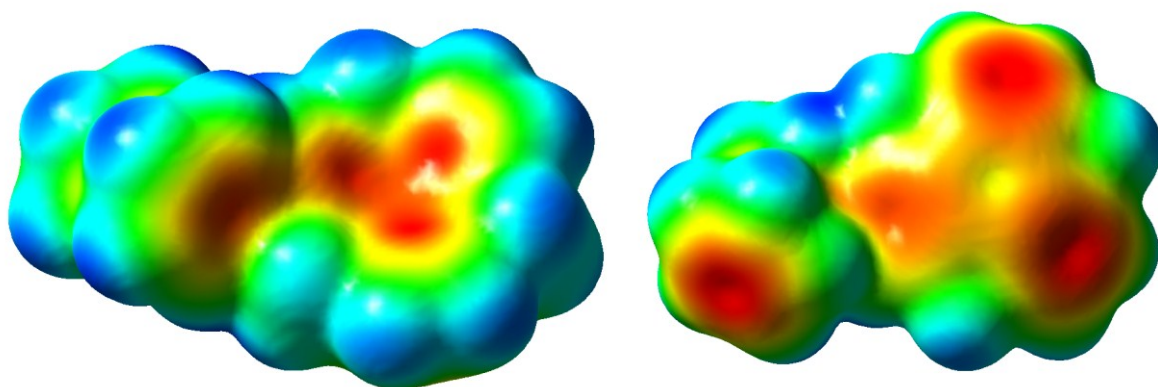


**Figure S13.** Electrostatic potential maps of **2**, view into the bowl (left) and from below (right)

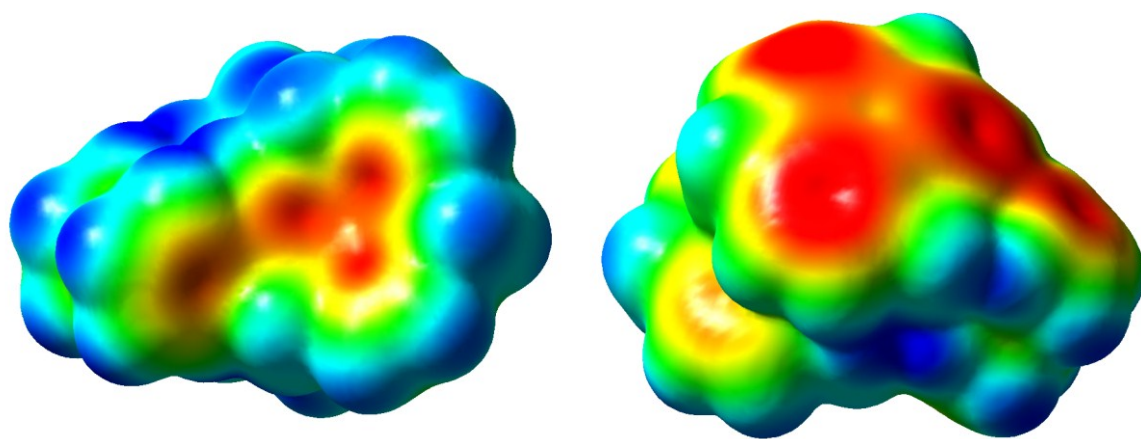


**Figure S14.** Electrostatic potential maps of **3**, view into the bowl (left) and from the side (right)

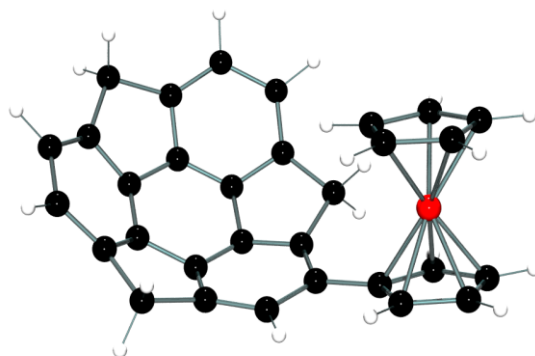


**Figure S15.** Calculated *endo-2*. Visualisation with Ortep3v2.

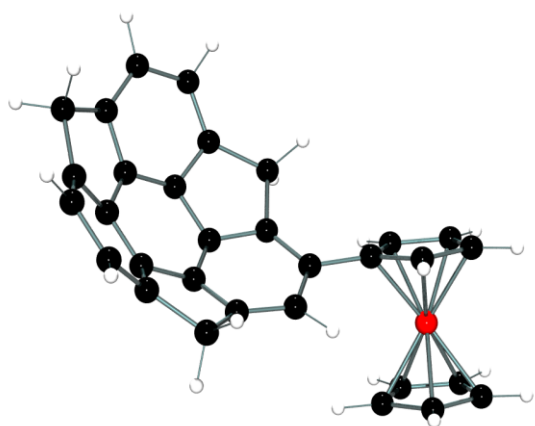


**Figure S16.** Calculated *exo-2*. Visualisation with Ortep3v2.

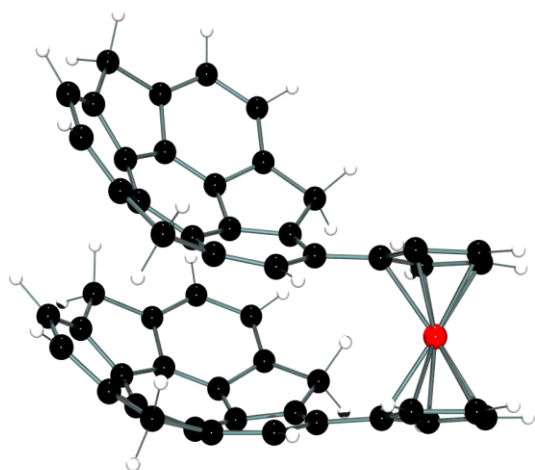


**Figure S17.** Calculated **3**. Visualisation with Ortep3v2.

## References:

- [S1] M. S. Inkpen, S. Du, M. Driver, T. Albrecht and N. J. Long, *Dalton Trans.*, 2013, **42**, 2813.
- [S2] Gaussian 09, Revision A.02, M. J. Frisch, G. W. Trucks, H. B. Schlegel, G. E. Scuseria, M. A. Robb, J. R. Cheeseman, G. Scalmani, V. Barone, B. Mennucci, G. A. Petersson, H. Nakatsuji, M. Caricato, X. Li, H. P. Hratchian, A. F. Izmaylov, J. Bloino, G. Zheng, J. L. Sonnenberg, M. Hada, M. Ehara, K. Toyota, R. Fukuda, J. Hasegawa, M. Ishida, T. Nakajima, Y. Honda, O. Kitao, H. Nakai, T. Vreven, J. A. Montgomery, Jr., J. E. Peralta, F. Ogliaro, M. Bearpark, J. J. Heyd, E. Brothers, K. N. Kudin, V. N. Staroverov, R. Kobayashi, J. Normand, K. Raghavachari, A. Rendell, J. C. Burant, S. S. Iyengar, J. Tomasi, M. Cossi, N. Rega, J. M. Millam, M. Klene, J. E. Knox, J. B. Cross, V. Bakken, C. Adamo, J. Jaramillo, R. Gomperts, R. E. Stratmann, O. Yazyev, A. J. Austin, R. Cammi, C. Pomelli, J. W. Ochterski, R. L. Martin, K. Morokuma, V. G. Zakrzewski, G. A. Voth, P. Salvador, J. J. Dannenberg, S. Dapprich, A. D. Daniels, Ö. Farkas, J. B. Foresman, J. V. Ortiz, J. Cioslowski, and D. J. Fox, Gaussian, Inc., Wallingford CT, 2009.